Article published online: 2021-07-30

Diffusion-weighted imaging in extracranial head and neck schwannomas: A distinctive appearance

Abanti Das, Ashu S Bhalla, Raju Sharma, Atin Kumar, Alok Thakar[1], Ankur Goyal

Departments of Radiodiagnosis and [1]Otolaryngorhinology, All India Institute of Medical Sciences, New Delhi, India

Correspondence: Dr. Ashu S Bhalla, Department of Radiodiagnosis, All India Institute of Medical Sciences, New Delhi - 110 029, India. E-mail: ashubhalla1@yahoo.com

Abstract

Purpose: To evaluate the diffusion weighted (DW) magnetic resonance imaging (MRI) features of the extracranial schwannomas of head and neck. **Materials and Methods:** The MRI (including DWI) of 12 patients with pathologically proven head and neck schwannomas (4 men, 8 women, with mean age of 32.6 years; age range 16–50 years) were retrospectively evaluated. Images were analyzed for signal intensity and morphology on conventional sequences followed by the qualitative evaluation of DW images (DWI) and measurement of apparent diffusion coefficient (ADC) values. **Results:** Majority of the tumors were located in the parapharyngeal space (8/12). All but one showed heterogeneous appearance, with 10 tumors showing scattered areas of hemorrhage. Eight out of 12 tumors showed intensely hyperintense core surrounded by intermediate signal intensity peripheral rim (reverse target sign) on T2-weighted (T2W) images. On DWI, these eight tumors showed a distinctive appearance, resembling target sign on trace DWI and reverse target on ADC map. Out of the remaining four tumors, one showed uniformly restricted diffusion whereas three showed free diffusion. Mean ADC value in the central area of free diffusion was 2.277×10^{-3} mm²/s (range of 1.790×10^{-3} to 2.605×10^{-3} mm²/s) whereas in the peripheral area was 1.117×10^{-3} mm²/s (range of 0.656×10^{-3} to 1.701×10^{-3} mm²/s). Rest of the schwannomas showing free diffusion had a mean ADC value of 1.971×10^{-3} mm²/s. **Conclusion:** Majority of the head and neck schwannomas showed a characteristic appearance of free diffusion in the centre and restricted diffusion in the periphery of the mass.

Key words: Benign; diffusion weighted imaging; head and neck neoplasms; magnetic resonance imaging; schwannoma

Introduction

Head and neck region is a common location for benign peripheral nerve sheath tumors which include schwannomas and neurofibromas, with the former being more common.[1] Although virtually any cranial, peripheral, or autonomic nerve can be involved, parapharyngeal space is the most common location of nonvestibular extracranial schwannomas. The detection of these tumors is often incidental as most of them are slow-growing. Surgical excision is the treatment of choice with the associated risks of postsurgical morbidity and neurological deficit. Because of their critical deep-seated location, imaging is often superior to clinical evaluation not only for their detection but also for differentiation from other possible mimickers.

Access this article online	
Quick Response Code:	Website: www.ijri.org
	DOI: 10.4103/0971-3026.184418

Cite this article as: Das A, Bhalla AS, Sharma R, Kumar A, Thakar A, Goyal A. Diffusion-Weighted Imaging in extracranial head and neck schwannomas: A distinctive appearance. Indian J Radiol Imaging 2016;26:231-6.

Although there is abundant literature on their imaging appearance on computed tomography (CT) and magnetic resonance imaging (MRI), the role of diffusion-weighted imaging (DWI) in their characterization has not been highlighted. Principal application of this technique in head and neck has been limited to the differentiation of benign and malignant entities, squamous cell carcinoma from lymphoma, and response evaluation post chemo- or radiotherapy. In addition, most of the published studies have been performed using 1.5T MR scanner. Imaging at 3T with dedicated 16-channel neurovascular coil can significantly improve the signal intensity-to-noise ratio, enabling better quality DWI and apparent diffusion coefficient (ADC) maps to be generated, which in turn can further improve the diagnostic performance.

Herein, we present MRI findings and highlight the DWI features of head and neck schwannomas evaluated on a 3T scanner.

Materials and Methods

This study to evaluate the DWI features of neck masses was conducted from July 2011 to January 2013 after approval by the institutional ethics committee. A total of 79 patients with a neck mass either on clinical evaluation or on any imaging modality were included in the study. Informed consent was obtained from all the patients. Among these 79 patients, there were 12 cases of schwannomas, which were confirmed either on histopathology ($n = 8$) or cytology ($n = 4$). This study is a retrospective evaluation of the MRI features including the DWI of these tumors.

MRI was performed on a 3T scanner (Achieva 3.0T TX Phillips, Netherlands) using 16-channel neurovascular coil with the patient in the supine position. Routine sequences included axial T1 weighted images (WI) (TR/TE 600-700/10-20 ms), axial and sagittal T2WI (TR/TE 3000-4000/70-90 ms), and coronal short *tau* inversion recovery (STIR). Post-gadolinium images were acquired in three participants. DWI were obtained in the axial plane using single-shot spin echo echo-planar technique (echo planar imaging factor: 67) using *b* values of 0, 500, and 1000 s/mm^2. Parameters used were: TR/TE 3400/86 ms, bandwidth: 2588.6 Hz/pixel, matrix: 152 × 121, section thickness: 4 mm with 0.4 mm intersection gap, field of view: 230–300 mm, flip angle: 90°, and resultant acquisition time of 2–3 min. Diffusion probing gradients were applied in three orthogonal planes. Trace DWI and ADC maps were automatically derived on a voxel-by-voxel basis at the workstation. Parallel imaging technique (sensitivity encoding, SENSE) with a SENSE factor of 2 was used in all the patients.

The images were reviewed by three radiologists in consensus (RS, ASB, and AK with 20, 15, and 11 years of experience with MRI, respectively). Routine MRI were evaluated for tumor location, size, margins, signal intensity on T1WI and T2WI, internal homogeneity, presence or absence of intracranial extension, and mass effect on adjacent structures. DWI in conjunction with ADC maps were evaluated both qualitatively (facilitated/restricted diffusion) and quantitatively. Lesions that showed drop in signal intensity with increasing *b* values from 0 to 500 and to 1000 s/mm^2, with corresponding hyperintense signal on ADC maps, were labelled as showing facilitated diffusion; whereas lesions that retained their signal or showed minimal decrease in signal on increasing *b* values and were hypointense on ADC maps were classified as showing restricted diffusion.

For quantitative assessment, circular regions of interest (ROIs) were drawn on the lesions to obtain representative ADC values. Multiple ROIs were drawn on the lesion and a mean of three such values was taken. For lesions showing uniform pattern of diffusion restriction or facilitation, ROIs were drawn on the most homogeneous part of the lesion while avoiding any obvious areas of hemorrhage/necrosis/artefacts. For lesions with an inhomogeneous appearance on DWI and ADC maps with prominent cystic areas, separate ROIs were drawn on both solid and cystic areas.

Results

The mean age of the patient cohort was 32.6 years (range of 16–50 years) with a male: female ratio of 1:2. All patients had solitary tumors and none of them had neurofibromatosis. Good quality images were obtained forall the patients. The mean long axis dimension of the schwannomas was 4.82 cm (range of 1.9–9.2 cm).

Majority of the tumors were located in the parapharyngeal space ($n = 8$), two were in parotid space and one each in masticator and posterior cervical space. Two of the lesions showed intracranial extension; one was a trigeminal schwannoma with extension to the Meckel's cave through foramen ovale, whereas another was a facial nerve schwannoma in parotid space extending to the petrous temporal bone via vertical mastoid segment of the facial nerve canal. All tumors had well-defined margins with round or fusiform configuration. None of the tumors showed vascular encasement.

On conventional MRI, all tumors were hypo- to isointense to adjacent muscle on T1WI images and heterogeneously hyperintense on T2WI. All but one tumor showed internal heterogeneity, with 10 tumors showing scattered areas of hemorrhage. Gadolinium was administered in three cases which showed intense heterogeneous enhancement of all the three masses. Tortuous vascular flow voids were noted in the periphery of one of the lesions.

A distinctive appearance on T2 weighted images, herein referred to as "reverse target" was noted in eight out of 12 schwannomas, which consisted of markedly hyperintense signal intensity in the central core surrounded by peripheral rind of solid tissue showing intermediate signal intensity [Figures 1 and 2]. The mean long axis dimension of this subgroup of tumors was 5.08 cm (range of 2.1–9.2 cm).

On DWI, a characteristic pattern of signal intensity was noted in the same eight tumors wherein peripheral areas retained signal on increasing *b* values and were hypointense on ADC maps suggestive of restricted diffusion; where as the central areas lost signal on increasing *b* values and were hyperintense on ADC maps suggestive of facilitated diffusion, which resembled target appearance on DWI trace images and reverse target on ADC map [Figures 1 and 2]. The mean ADC value in peripheral areas was 1.117×10^{-3} mm^2/s (range of 0.656×10^{-3} to 1.701×10^{-3} mm^2/s) and that of central areas was 2.277×10^{-3} mm^2/s (range of 1.790×10^{-3} to 2.605×10^{-3} mm^2/s).

Of the remaining four tumors, three showed facilitated diffusion [Figure 3] whereas one showed restricted diffusion [Figure 4]. Mean ADC value of tumors with only facilitated diffusion was 1.971×10^{-3} mm^2/s (range of 1.991×10^{-3} to 1.983×10^{-3} mm^2/s) whereas that of tumor with only restricted diffusion was 1.238×10^{-3} mm^2/s. Figure 5 summarizes the diffusion characteristics of the schwannomas seen in our study.

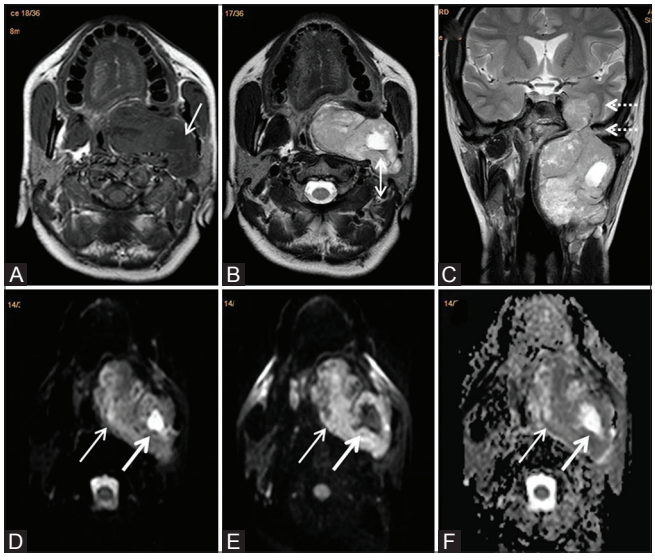

Figure 1 (A-F): A 32-year-old female with left trigeminal nerve schwannoma. Axial T1 weighted image (A) showing well-defined left parapharyngeal space mass, isointense to muscle, with few internal hypointense areas (white arrow). Axial T2 weighted image (B) showing heterogeneous mass with markedly hyperintense centre and relatively isointense periphery. Blood fluid level noted in central hyperintense area (double ended arrow). Coronal T2 weighted image (C) showing intracranial extension via left foramen ovale (dashed arrows). Diffusion-weighted images at $b = 0$ (D), $b = 1000$ (E) s/mm^2, and ADC map (F) reveal marked restriction at the peripheral rim of the tissue (thin arrows) with free diffusion in the centre (thick arrows)

Discussion

Approximately 45% of benign peripheral nerve sheath tumors occur in the head and neck region.[2] Their indolent clinical course and consideration of postoperative neurological sequelae warrant an accurate initial diagnosis as well as exclusion of other possible entities.

Almost all the schwannomas in our series had a heterogeneous appearance. This can be attributed to cystic degeneration, xanthomatous changes, and mixed areas of relative hypo- and hypercellularity, which are frequently seen in schwannomas.[3] We report a characteristic appearance of schwannomas on MRI—"reverse target" on T2W images, "target" on high b value DW trace image, and "reverse target" on ADC map, which was seen in eight out of 12 patients in our series (66.67%). The peripheral areas of restricted diffusion corresponded to the solid areas of tumor (intermediate signal intensity on T2WI) whereas central areas of free diffusion (markedly hyperintense areas on T2WI) were suggestive of necrosis or cystic degeneration [Figures 1 and 2]. This characteristic pattern of differential diffusion characteristics in the central and peripheral parts of the same tumor was noted irrespective of tumor size.

Target sign on T2WI was initially described for neurofibromas and was seen as low-to-intermediate signal intensity in the centre with peripheral high signal intensity.[4,5] The pathological correlate for this imaging appearance was the presence of fibrous tissue and hypercellular Antoni type A bodies in the centre and relatively hypocellular Antoni type B bodies at the periphery.[4] Subsequent studies showed the presence of this appearance in schwannomas as well.[4,6,7] However, we did not come across any literature on reverse target sign on T2W images in schwannomas.

Diffusion characteristics of schwannomas have been infrequently described in the literature and there is no uniform consensus on their behaviour on DWI. Sener *et al*.[8] reported facilitated diffusion in a series of six

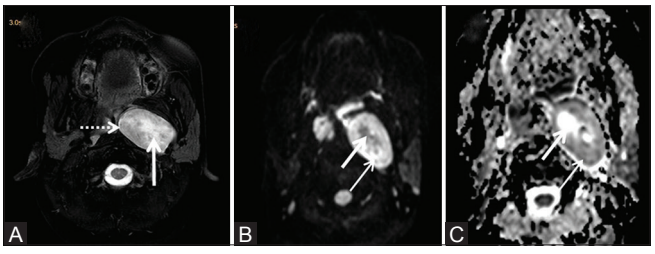

Figure 2 (A-C): A 35-year-old female with left parapharyngeal space schwannoma. Axial T2 weighted fat-saturated image (A) showing well-defined heterogeneously hyperintense mass in the left parapharyngeal space. Central area of the lesion (double ended arrow) is more hyperintense than the peripheral (dashed arrow). Diffusion-weighted image at $b = 1000$ (B) s/mm^2 and ADC map (C) show restriction at the peripheral rim of the tissue (thin arrows) with free diffusion in the centre (thick arrows)

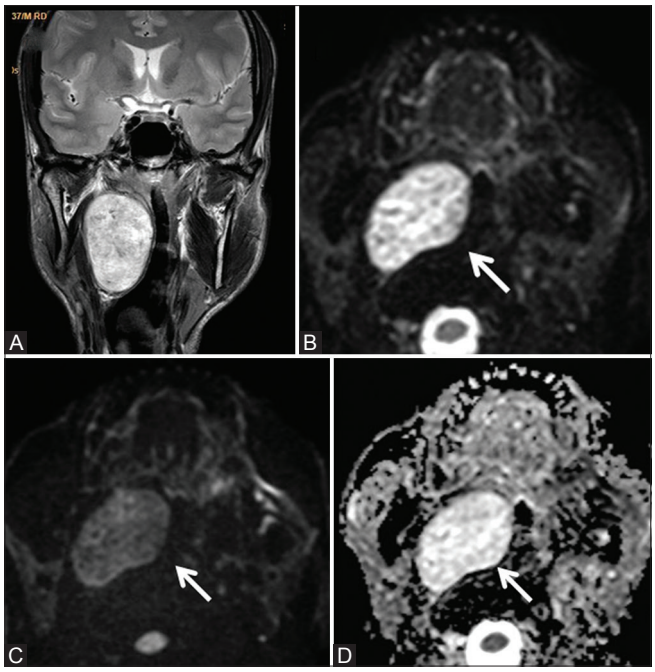

Figure 3 (A-D): A 37-year-old man with right parapharyngeal space schwannoma. Coronal T2 weighted image (A) shows fusiform shaped mass in the right parapharyngeal space with heterogeneous hyperintense signal intensity. No central necrosis seen. Diffusion weighted images at b = 0 (B), b = 1000 (C) s/mm^2, and ADC map (D) show free diffusion throughout the mass (thick arrows)

solid vestibular schwannomas, which was seen in three of our schwannomas, suggestive of relatively loose acellular tumor matrix. On the other hand, there are isolated solitary case reports each of benign rectal[9] and gastroduodenal ligament schwannoma[10] documenting restricted diffusion, as was noted in one facial nerve schwannoma in our series. The diffusion characteristics of nerve sheath tumors published in previous studies are shown in Table 1.

As is evident from above, no large-scale study has been done to conclusively establish the nature of diffusion characteristics of head and neck schwannomas. Nevertheless, all the limited available studies conform to the heterogeneous morphology of these lesions, which can, to some extent, explain the wide variability of tissue diffusivity. Only one of the studies mentions the presence of a "target sign" in 2/21 lesions on DWI;[14] however, no further description of the appearance or explanation for this appearance is available.

We report a novel observation which has not been described previously and is actually a reverse of the previously described "target sign" in nerve sheath tumors on T2WI.[4,5] The possible explanation for such an imaging appearance is as follows.

ADC value in mono exponential model is a function of both molecular diffusion and capillary perfusion. However,

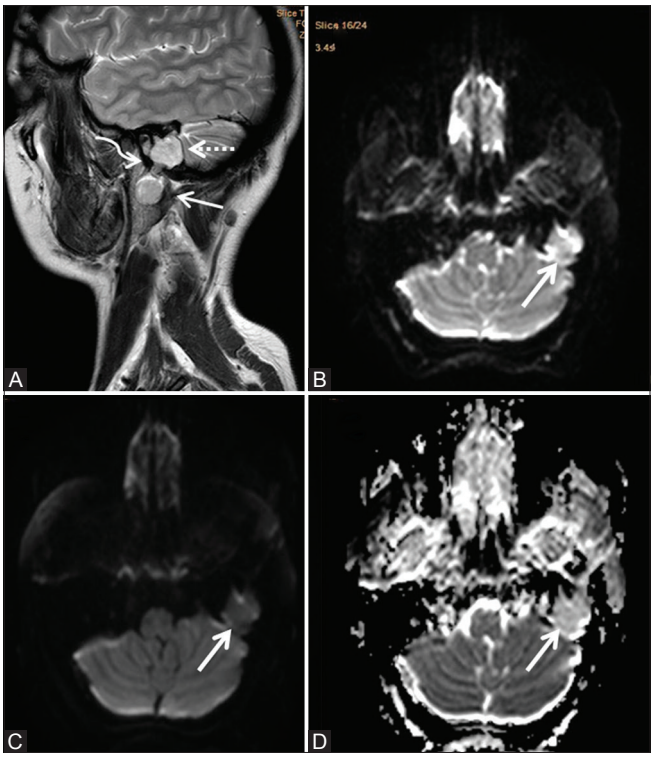

Figure 4 (A-D): A 32-year-old female with left facial nerve schwannoma. Sagittal T2 weighted image (A) showing hyperintensebilobed mass in the left parotid region (thin arrow) and the left mastoid region (dashed arrow). Interconnecting stalk seen along the vertical (mastoid) segment of facial nerve (squiggly arrow). Diffusion-weighted image at b = 0 (B), b = 1000 (C) s/mm^2, and ADC map (D) show restricted diffusion in the lesion (thick arrows)

because the central area of the tumors did not enhance on post contrast images in all three of our patients in whom gadolinium was administered, the observed high ADC values in the central part of the tumor can be ascribed only to high diffusion component. This high diffusivity may be due to loose acellular matrix or hypo cellular Antoni type B areas in the centre. Large tumors may outgrow their blood supply and undergo central necrosis.[18] However, the presence of this distinctive appearance, irrespective of tumor size in our series, suggests that the aforementioned general hypothesis may not be responsible for this appearance.

To the best of our knowledge, this unique appearance of schwannomas on T2WI and DWI has not been previously described. Whether this appearance is unique to head and neck schwannomas, needs further studies for validation.

A major limitation of our study was the small patient population. In addition, the study group did not have any neurofibromas or malignant nerve sheath tumors to compare the diffusion characteristics. This was because our study group was targeted to all head and neck masses, and current retrospective study includes only a subset of patients with pathologically confirmed schwannomas.

Table 1: Summary of previous studies on diffusion-weighted imagingin nerve sheath tumors

Author	Year	Field strength (T)	No. of lesions†	Study cohort	DWI
van Rijswijk CS *et al*.[11]	2001	1.5	23 (2)	Extremity soft tissue tumors	*b*: 0,176,351,526,701 s/mm^2 ADC: 1.36, 1.95×10^{-3} mm^2/s
Sener[8]	2003	1.5	6 (6)	Vestibular schwannoma	*b*: 1000 s/mm^2 high mean ADC compared to normal brain parenchyma (1.42±0.17×10^{-3} mm^2/s)
Srinivasan *et al*[12]	2008	3.0	33 (6)	Head and neck masses	*b*: 0,800 s/mm^2 variable ADC values: 0.739-2.080×10^{-3} mm^2/s
Khedr *et al*[13]	2012	1.5	73 (5)	Extremity masses	*b*: 0,176,351,526,701 s/mm^2 Mean ADC of Schwannomas: 1.5±0.19×10^{-3} mm^2/s
Fayad *et al*[14]	2013	3.0	23 (6)‡	Extremity lesions in NF-2 and Schwannomatosis	*b*: 50, 400, 800 s/mm^2 Variable ADC: 0.8-3.9×10^{-3} mm^2/s
Chhabra *et al*[15]	2013	3.0	30 (16)	Extremity nerve tumor and tumor-like conditions	*b*: 50, 400, 800 s/mm^2 (DWI); 0,800, 1000 s/mm^2 (DTI) ADC not statistically different (P>0.05; benign, 1.745±0.44×10^{-3} s/mm^2 versus malignant, 1.267±0.35×10^{-3} s/mm^2)
Sumi *et al*[16]	2014	1.5	92 (6)	Head and neck tumors	*b*: 0,500,1000 s/mm^2 D (molecular diffusion):≥1.2×10^{-3} mm^2 PP (Perfusion parameter):≥0.17
Demehri *et al*[17]	2014	3T	31 (14)	Extremity nerve sheath tumors	*b*: 50, 400, 800 s/mm^2 Minimum ADC ≤1×10^{-3} mm^2/s

†Numbers in parenthesis indicate the number of schwannomas in the study group. ‡Study population had onepatient of schwannomatosis with sixschwannoma. DWI: Diffusion weighted imaging

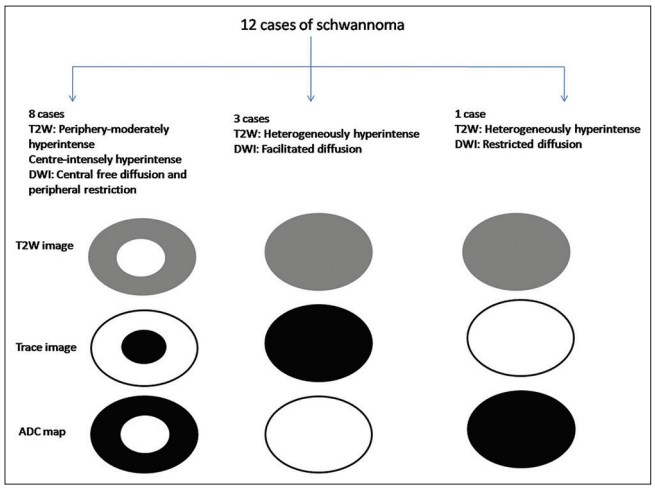

Figure 5: Schematic diagram showing T2 weighted imaging appearance and diffusion characteristics of extracranial head and neck schwannoma

For the same aforementioned retrospective nature of this study, exact histopathological correlate corresponding to the different sections of the lesion showing differential diffusion characteristics was not available. Nevertheless, this study presents the DWI appearance of the largest cohort of extracranial head and neck schwannomas with excellent image quality by virtue of high field strength imaging at 3T.

Conclusion

We here by report a distinctive pattern of appearance on T2WI and DWI in extracranial head and neck schwannomas—"reverse target" on T2W images, "target" on high b value DW trace image and "reverse target" on ADC map. This appearance, seen irrespective of tumor size, corresponds to intensely hyperintense core surrounded by the peripheral rim of intermediate signal intensity on T2WI, and central free diffusion surrounded by peripheral restriction on DWI. Knowledge of such unique appearance on MRI can have potential diagnostic value in equivocal cases.

Financial support and sponsorship
Nil.

Conflicts of interest
There are no conflicts of interest.

References

1. Colreavy MP, Lacy PD, Hughes J, Bouchier-Hayes D, Brennan P, O'Dwyer AJ, *et al*. Head and neck schwannomas-A10 year review. J Laryngol Otol 2000;114:119-24.
2. Das Gupta TK, Brasfield RD, Strong EW, Hajdu SI. Benign solitary schwannomas (neurilemomas). Cancer 1969;24:355-66.
3. Cohen LM, Schwartz AM, Rockoff SD. Benign schwannomas: Pathologic basis of CT inhomogeneities. Am J Roentgenol 1986;147:141-3.
4. Suh JS, Abenoza P, Galloway HR, Everson LI, Griffiths HJ. Peripheral (extracranial) nerve tumors: Correlation of MR imaging and histologic findings. Radiology 1992;183:341-6.
5. Jee WH, Oh SN, McCauley T, Ryu KN, Suh JS, Lee JH, *et al*. Extraaxialneurofibromas versus neurilemmomas: Discrimination with MRI. Am J Roentgenol 2004;183:629-33.
6. Murphey MD, Smith WS, Smith SE, Kransdorf MJ, Temple HT. From the archives of the AFIP. Imaging of musculoskeletal neurogenic tumors: Radiologic-pathologiccorrelation. Radiographics 1999;19:1253-80.
7. Anil G, Tan TY. CT and MRI evaluation of nerve sheath tumors of cervical vagus nerve. Am J Roentgenol 2011;197:195-201.
8. Sener RN. Diffusion magnetic resonance imaging of solid vestibular schwannomas. J Comput Assist Tomogr 2003;27:249-52.

9. Tan ACH, Tan CH, Nandini CL, Ng CY. Multimodality Imaging Features of Rectal Schwannoma. Ann Acad Med Singapore 2012;41:476-8.
10. Bayraktutan U, Kantarci M, Ozgokce M, Aydinli B, Atamanalp SS, Sipal S. Gastrointestinal: Benign cystic schwannoma localized in the gastroduodenal ligament; Arare case. J Gastroenterol Hepatol 2012;27:985.
11. van Rijswijk CS, Kunz P, Hogendoorn PC, Taminiau AH, Doornbos J, Bloem JL. Diffusion-Weighted MRI in the Characterization of Soft-Tissue Tumors. J Magn Reson Imaging 2002;15:302-7.
12. Srinivasan A, Dvorak R, Perni K, Rohrer S, Mukherji SK. Differentiation of benign and malignant pathology in the head and neck using 3T apparent diffusion coefficient values: Early experience. Am J Neuroradiol 2008;29:40-4.
13. Khedr SA, Hassan MA, Abdelrazek NM, yehia Sakr A. Diagnostic impact of echo planar diffusion-weighted magnetic resonance imaging (DWI) in musculoskeletal neoplastic masses using apparent diffusion coefficient (ADC) mapping as a quantitative assessment tool. Egyptian J Radiol Nuc Med 2012;43:219-26.
14. Fayad LM, Blakeley J, Plotkin S, Widemann B, Jacobs MA. Whole Body MRI at 3T with Quantitative Diffusion Weighted Imaging and Contrast-Enhanced Sequences for the Characterization of Peripheral Lesions in Patients with Neurofibromatosis Type 2 and Schwannomatosis. ISRN Radiol 2013:627932.
15. Chhabra A, Thakkar RS, Andreisek G, Chalian M, Belzberg AJ, Blakeley J, *et al*. Anatomic MR Imaging and Functional Diffusion Tensor Imaging of Peripheral Nerve Tumors and Tumorlike Conditions. Am J Neuroradiol 2013;34:802-7.
16. Sumi M, Nakamura T. Head and neck tumors: Combined MRI assessment based on IVIM and TIC analyses for the differentiation of tumors of different histological types. Eur Radiol 2014;24:223-31.
17. Demehri S, Belzberg A, Blakeley J, Fayad LM. Conventional and Functional MR Imaging of Peripheral Nerve Sheath Tumors: Initial Experience. Am J Neuroradiol 2014;35:1615-20.
18. Hughes MJ, Thomas JM, Fisher C, Moskovic EC. Imaging features of retroperitoneal and pelvic schwannomas. Clinical Radiology 2005;60:886-93.